Correspondence between different view breast x-rays using curved epipolar lines

Yasuyo Kita Ralph Highnam Michael Brady

Intelligent Systems Division
Electrotechnical Laboratory
Tsukuba, Japan 305-8568

Dept. of Engineering Science
University of Oxford
Oxford,UK OX1 3PJ

Abstract

In this paper, we propose a method for matching a deformable object between time-varying stereo images. This method has been developed primarily to find correspondences between a cranio-caudal (CC) (head to toe) and a medio-lateral oblique (MLO) (shoulder to the opposite hip) x-ray mammogram of the same breast.The two mammograms are taken while the breast is compressed between the cassette and plate of the x-ray machine. This results in a different amount of compression in each direction. The deformations of the breast caused by the different compressions cause corresponding points to appear far from straight "epipolar lines" familiar from binocular stereo vision. The method developed in this paper calculates the curve in a MLO image corresponding to a point in the CC image through simulation of the differential deformation and the projection of a 3D curve corresponding to the point. Experiments on real data show that the method predicts well the corresponding position in the other image. We also illustrate the program's ability to estimate the 3D position of a lesion in the uncompressed breast.

Short running head: Correspondence using curved epipolar lines

The person to whom correspondence should be sent:

Yasuyo KITA
Intelligent Systems Division, Electrotechnical Laboratory,
1-1-4 Umezono, Tsukuba, Ibaraki 305-8568, Japan
Email:ykita@etl.go.jp tel:+81-298-61-5957 fax:+81-298-61-5961

List of the symbols used in the paper

i_s^{CC} j_s^{CC} i_n^{CC} j_n^{CC} i_n^{MLO} j_n^{MLO}
l l_u L L'_u L_u
$P_m(m = 1 \sim 4)$ $L_m(m = 1 \sim 3)$ x_{P_4}
P_u P_c P_l P'_u P'_l C_a x_c
C_k P_{k1} x_k y_{k1} P_{k2} y_{k2} P_{k3} z_{k3}
P_{k4} z_{k4}
P_u^{CC} P_l^{CC} y_{source}^{CC} L^{CC}
a $IHEIGHT$ H^{CC}
$P'_k(x'_k, y'_k, z'_k)$ $P''_k(x''_k, y''_k, z''_k)$
y_c P_0 θ
$P'_{u,k}$ $P''_{u,k}$ $P'_{c,k}$ $P'_{l,k}$ $P''_{l,k}$
L^{MLO} H^{MLO} $i_n'^{MLO}$ $j_n'^{MLO}$ y'^{MLO}_{source}
$i_k'^{MLO}$ $j_k'^{MLO}$ i_k^{MLO} j_k^{MLO}

1 Introduction

Mammography (breast x-ray) is currently the best way to detect breast cancer in its early stages, at least for older women. As a result, screening programmes have been established in a number of countries, such as the UK, Netherlands, Sweden, and Australia. Currently, screening programmes are being established in France, Germany, and Japan. Most programmes require that a single image be taken in the medio-lateral oblique (MLO) direction since that view has been shown to be optimal with regards to the amount of breast imaged and because it is most likely to enable axial involvement to be seen (indicative of metastasis). However, it has recently been proposed that performing two different views of the breast, the medio-lateral oblique and cranio-caudal (CC), may greatly improve sensitivity and specificity. In the UK, it is policy to take both CC and MLO views since it has been shown that it substantially reduces the number of false positives (cancers flagged erroneously) and false negatives (missed cancers). When a mammogram is performed, the breast is compressed between the film-screen cassette and compression plate in the direction of the x-ray source (analogically, camera direction): "head to toe" for the CC view and "over the shoulder diagonally to the hip" for the MLO view, as shown in Figure 1[1]. Breast compression is necessary for many reasons, most importantly to reduce the x-ray dose administered to the breast tissue. It also has the benefit of spreading breast tissue laterally, which reduces the occurrence of overlapping structures in what is intrinsically a projective process. Unfortunately, radiologists find it difficult to relate points in the CC view to those in the MLO view. The technique reported in this paper contributes to enhancing their ability to match the two mammograms that they are increasingly required to take.

Fusing the information provided by the two views requires in turn that corresponding points be found in the two images. One approach for determining the correspondences between the views is to apply 2D-2D image feature matching[2]. However, such an approach can not be used in its customary form because the image intensities that form a mammogram vary considerably for many reasons two of which are the amount of breast compression and the time-of-exposure. The recent monograph by Highnam and Brady describes in detail the formation of a mammogram[3].

In mammography, the x-ray source and the film can be thought of as the focus and the image plane of a pin-hole camera system. The x-ray source and the film move rigidly as shown in Figure 1d so that the camera direction remains constant relative to the image plane. Since the CC and the MLO image are taken from different camera directions, the correspondences between the CC and the MLO images are related to the geometry of stereo vision[4]. It is well-known that given a point on an object in one image it is possible to define a straight line in the other image which marks where the object must lie. That line is termed the "epipolar line".

However, binocular stereo vision techniques can not be applied straightforwardly, since the breast is an elastically deformable object that is compressed to different extents in different directions for the two views. The differential compression substantially impacts on the stereo matching problem. Because of the deformation of the breast tissue in the two images, a point in a CC image that in fact corresponds to a particular point in the MLO image often appears far from the epipolar line that would be constructed based on the assumptions of stereo vision. Such deviations vary according to the 3D position of the point of interest, typically corresponding to a lesion (e.g. cancer). Compression and the 3D nature of the breast also make it difficult for expert radiologists to say with certainty (or reasonable accuracy) where they expect a sign in one view to appear in the other. Indeed, these same problems also hinder previously published techniques for calculating the correspondences between different views of mammograms[5][6] since they do not explicitly address those problems.

The solution that is proposed in this paper is to calculate curved epipolar lines by developing a simulation of object deformation into the stereo camera geometry. Using such curved epipolar lines, we can not only determine correspondences, but can estimate the 3D location of a lesion within the uncompressed breast.

We start the paper by describing our methods, which first overviews our strategy for matching. We present a simplified model of breast compression and outline the entire process of matching. We then present results in which we conduct many experiments using actual examples to examine the accuracy of the proposed method. Note that a richer compression model could easily be substituted for the model developed in this paper, and indeed we are continuing to work in this area. We end with a number of conclusions.

2 Overview of determining correspondences

2.1 Strategy for stereo vision of a deformable object

Even though we are analyzing 2D images of a deformable object, the images are the result of 3D phenomena such as the transformation and projection of the object and so it is natural and sensible to consider these factors in 3D space. Furthermore, since the problem is relatively constrained, a model-based approach is plausible. A deformable model-based method based on this approach has already successed in the analysis of stomach x-ray images[7] and the monograph by Highnam and Brady [3] argues the merits of this approach more generally in medical image analysis, particularly mammography.

In this paper, we propose to introduce a deformable model-based approach into the camera geometry for stereo vision applied to a deformable object. Figure 2a overviews the principle. In familiar binocular stereo vision, the epipolar line, that is the corresponding line in the other image, is calculated through simulation of the projection process. More precisely, it is obtained by projecting the 3D corresponding line which is the locus of possible 3D positions of a point in the first image in the second image. As the object is deformed between the first and the second images, the corresponding 3D line is also deformed. As a result, the "correct" corresponding line is manifest as a distorted "epipolar line". To calculate the curved epipolar line, we introduce a simulation of the deformation before projecting the 3D line onto the second image.

2.2 Curved epipolar lines of breast x-rays

When we attempt to apply this strategy to compute correspondences of breast CC and MLO x-ray images, the key step is to determine how to simulate the object deformation. In the continuing absence of a precise model of breast tissue compression, in this paper we use a mixture of qualitative and quantitative knowledge. Figure 2b shows the five steps of the process: after taking the first image (CC) the breast is uncompressed into its estimated natural shape and it is again compressed in a different direction to take

the second (MLO) image.

There are two main difficulties to be taken into account:

1. simulation of the large deformation of a soft object is still an open problem.
2. most of boundary conditions for the simulation are not known accurately.

Although recently deformable models have begun to be developed in medical image analysis[8], there is little research which simulates physical deformation using deformable models. Even in heart motion tracking[9], the forces used to deform the models are not genuine ones but ones determined so as to attract the object to observed image features or 3D data. To simulate actual physical deformations, both the force exerted to the object and the viscoelasticity of the object need to be known, though these are not straightforward to determine in practice (without laboriously applying a device such as a linear voltage displacement transducer across the breast). Note that the complex ligament structure of the breast means that the internal strain tensor is far from being isotropic, as is supposed by most researchers. Additionally, volumetric deformable models which are essential for implementation of deformation are still in the earliest stages of research. For example, in heart motion tracking[9], volumetric deformable models are studied; but these are extensions of surface models for surfaces with thickness.

The simulation of breast deformation includes difficult problems such as the necessity for a general volumetric deformable model, irregularity of the deformation and non-uniform boundary conditions, that is, the connection to the chest wall. Additionally, breasts exhibit massive variations in shape and each 3D shape is not known precisely. Finally, the way in which a radiographer positions the breast between the plates affects the deformation but there is little information about this (especially for old mammographic machines) other than the guidelines written by quality control organizations.

Our initial approach to realize an analytical simulation under such conditions is to produce a simplified deformation process model. For example, the integrative analysis of several x-ray images of the stomach[7] obtained good correspondences of a deformable stomach between images by making appropriate simplifications to what are, in reality, complicated and unknown factors. For appropriate simplification, it is important to understand the principle of the object deformation, here, breast deformation under compression. There are several clinical studies which consider how a lesion appears in an x-ray image based on the projective principle[10],[11]. Perhaps the most comprehensive study to date is that by Novak[11] who studied deformations of the breast surface during compression by observing the movements of marks made on the skin of volunteers' breasts. Although such observations only give information about skin movement, and do not strictly give information about movements of tissue internal to the breast, the knowledge gleaned from these experiments aids understanding of the complicated deformation of a breast and, equally importantly, provides insight into the variations of such deformations across the population.

3 Simplification of deformation

3.1 Preconditions

First, we establish a set of 3D breast coordinates. Although Sickles[6] used 3D coordinates and considered orthogonal projections of microcalcifications, which are small flecks of calcium and/or magnesium salts and which are often the earliest signs of cancer[3], the coordinates were not established precisely because the breast deformation was not considered in 3D space. Since, we are directly concerned with breast deformation, the 3D coordinates are defined more carefully and are based on the uncompressed breast. To eliminate the considerable effect of gravity on the intrinsic shape of the breast, the canonical shape of the breast is defined to be that which it would have if it were to be pulled gently away from the chest wall, so that the nipple is the point furthest from the chest wall. The chest wall in the vicinity of the breast approximates a vertical plane. The origin of the coordinate system is defined to be the foot of the perpendicular from the nipple to the chest wall; this perpendicular is chosen to be the x-axis. The z-axis lies in the plane of the chest wall in the vertical (gravity) direction. Finally, the y-axis completes the left-handed coordinate system, and is the horizontal along the chest wall. According to established guidelines for taking mammograms[1][10], the breast is pulled gently away from the chest wall so that all tissues can be seen without any folding. This implies that the nipple hardly moves under compression relative to the origin for all

mammograms and it approximately maintains its 3D coordinates relative to the original state. In terms of this system of coordinates, the camera direction (x-ray source direction) for CC images is the z-axis. To take an MLO image of the right (left) breast, the camera is rotated through an unknown angle that is typically in the range $30 \sim 60$ ($-30 \sim -60$) degrees around the x-axis.

For the problem that we are attempting to solve, we assume that we are given the image coordinates of an "interesting point" in the CC image $(i^{CC}_{s(tarting)}, j^{CC}_{s})$ and we further suppose that we know the coordinates of the nipple in both the CC (i^{CC}_{n}, j^{CC}_{n}) and the MLO images $(i^{MLO}_{n}, j^{MLO}_{n})$. The image coordinates are defined so that the i and j axes are parallel to the x and y axes respectively and the upper left corner of the image is the origin (0,0). We also assume that we are given the breast outlines in the images. Although the nipple coordinates and the outlines are extracted manually, in related work we have developed automatic techniques to effect accurate segmentations[3]. In fact, extracting the profile is relatively straightforward.

3.2 Compression model

From now on, we abbreviate the breast compression while taking the CC image as the "CC-compression", similarly for "MLO-compression". We refer to the cross-section cut by the plane which is parallel to the compression direction and perpendicular to the chest wall as "the cross-section for compression". Figure 3 shows such a cross-section for CC-compression. The movement of each point of the breast by compression is expected to be largest in the cross-section. Therefore, for simplification, we ignore the element perpendicular to the cross-section and consider only the deformation of the breast within each cross-section.

Approximation 1(A1). The cross-section for compression of the breast is deformed only in the plane by compression.

Noting that, to a very good approximation, the pressure caused by the two parallel plates (the compression plate and the cassette) of the x-ray machine is uniform, it is reasonable to suppose that the forces from the two plates counterbalance each other in the plane parallel to the two plates and midway between them and that the deformation is small in the central plane. Following this observation, a second approximation is adopted:

Approximation 2(A2). In the mid-plane between the plate and the cassette, there is no deformation.

From the established guidelines for performing mammograms[1][10], all images are taken so that the nipple lies in the mid-plane between the plate and the cassette. Based on **Approximation A2**, the nipple does not change its position and so maintains the same coordinate and is on the x-axis.

We also make an approximation concerning the stretching (shrinking) of the breast tissue. The approximation is for each line of tissue through the breast and does not take into consideration volume conservation.

Approximation 3(A3). If a curve of breast tissue deforms, then it does so uniformly, that is, it stretches or shrinks by a constant factor of its curvilinear coordinate.

Using these approximations, the position of a point on the skin under compression can be calculated from its original position, and vice versa, if the original breast shape and the thickness at the compressed state is known. The shape of the compressed breast in the cross-section approximates to a rectangle whose height is the thickness of the compressed breast and whose width is the distance between the chest wall and the intersection of the breast contour and the plane $z = 0$ (P_4 in Figure 3). Consider one point on the upper contour, P_u, and its movement to P'_u under compression. Based on **Approximation A3**, the upper contour P_1P_4 (see Figure 3 for $P_m (m = 1 \sim 4)$), whose length is L_u, is uniformly stretched to have length, $L'_u = L_1 + L_2 + L_3$. Here, L_m represents the length of $P_mP_{(m+1)}$. Therefore, the x and z coordinates of P'_u, x'_u and z'_u are determined by the length P_1P_u, l_u, as follows:

$$
\begin{array}{l}
l = l_u * L'_u / L_u, \\
x'_u = 0 \qquad z'_u = (L_1 + L_3) - l; \quad if(l \le L_1) \\
x'_u = l - L_1 \quad z'_u = L_3; \quad if(L_1 < l \le (L_1 + L_2)) \\
x'_u = x_{P_4} \qquad z'_u = L'_u - l; \quad if((L_1 + L_2) < l)
\end{array}
$$

where x_{P_4} is the x coordinate of P_4.

Next, we consider deformations inside the breast. Suppose a vertical line penetrates inside the breast as shown in Figure 3. Denote the intersections with the upper contour, with the plane $z = 0$, and with the

lower contour by P_u,P_c and P_l. By **Approximation A2**, P_c maintains its position. Generally, P'_u and P'_l, which are the points on the compressed breast corresponding to P_u and P_l, move towards the chest wall. By smoothly connecting the three points, we deduce that the vertical line deforms into an arc which protrudes from the chest wall to the nipple. The exact shape of the curve is not known as well as it could change depending on the individual breast parameters (e.g. shape, stiffness of the tissue). Lacking a better model, we propose here simply to represent the curve as follows:

Approximation 4(A4). The curve $P_c\ P'_u$ and the curve $P_c\ P'_l$ are represented respectively by quadratic equations.

More precisely, in the CC-compression case, $x = C_a z^2 + x_c$ where, x_c is the x coordinate of P_c, and C_a is the constant that forces the curve to go through $P'_{u(l)}$.

Although we have explained these simplifications in the case of CC-compression, we can apply them to compressions in all directions.

3.3 3D breast reconstruction

As we saw in the previous section, for the calculation of the deformation:
1)the original(uncompressed) breast shape,
2)the breast thickness under compression
are required to calculate the shift of a point in the breast caused by the compression. The thickness of the breast under compression can be calculated using the intensity of each image and system calibration data [12]. The 3D breast shape can be roughly reconstructed from the outlines of the breast in the CC and the MLO images as follows.

Firstly, note that the CC image is the projection from the z-axis direction. Since the breast contour from that direction lies in the mid-plane between the plate and the cassette (the plane of $z = 0$) and hardly deforms under the CC-compression (**A2**), the outline in the CC image approximately shows the contour of the original breast at the plane of $z = 0$. If we have the medio-lateral (ML) or the latero-medial (LM) images which are taken from the direction of the y-axis, the contour of the breast at the plane of $y = 0$ is similarly shown as the outline. In the case of the MLO image, the situation is not so simple since the breast contour in the camera direction for the MLO image does not lie in the mid-plane and is deformed by compression. However, we have studied the breast contours of real mammograms and have observed that the contours of MLO images are very similar to those of ML(or LM) images. Therefore we approximate the contour in the plane $y = 0$ with the outline of the MLO image.

Figure 4a,b shows an example of the two contours. Since not all parts of the outline are observed on the images, mainly because of overlap by the arm, the part(the dashed lines in Figure 4b) is extrapolated by simple extension from the tangent of the adjoining part of the observed outline. On each plane $x = C_k$, we know the positions of four points on the breast skin, $P_{k1}(x_k, y_{k1}, 0)$, $P_{k2}(x_k, y_{k2}, 0)$, $P_{k3}(x_k, 0, z_{k3})$ and $P_{k4}(x_k, 0, z_{k4})$ from the two contours. Using the four positions, the cross-section of the breast at $x = C_k$ is reconstructed with two semi-ellipses, one of which is fixed by the three points, P_{k1}, P_{k3} and P_{k2} and the other fixed by P_{k1}, P_{k4} and P_{k2}. Figure 4c shows the result of the 3D reconstruction.

4 Step-by-step matching process

In this section, we follow the entire simulation process to calculate a curved epipolar line according to the diagram of Figure 2b. Although we explain the processes using the case to determine a curved epipolar line in the MLO image corresponding to a given point in the CC image, the method is completely reversible.

A) Reconstruction of a 3D line under CC-compression

First, we reconstruct the three 3D points, P_u^{CC}, P_c, and P_l^{CC} in Figure 5, on the line connecting the interesting point, (i_s^{CC}, j_s^{CC}), to the x-ray source. The x-ray source lies just above (0, IHEIGHT/2.0) of an x-ray image with the distance of L(=65cm) from the film, where IHEIGHT is the height of the x-ray image. Therefore, the three-dimensional coordinates of the x-ray source is $(0, y_{source}^{CC}, L^{CC})$, where $y_{source}^{CC} = a(IHEIGHT/2.0 - i_n^{CC})$ with a, the pixel size, and $L^{CC} = L - H^{CC}/2$ with H^{CC}, the thickness of the breast under CC-compression. The 3D coordinates of the nipple P_n and P_u^{CC}, P_c, P_l^{CC} can be calculated based upon the perspective projection principle.

B)Calculation of deformation by uncompression

Since the distance from the image plane is typically 65cm which is large compared to the typical

compressed breast size of between 4 and 7cm, the line $P_u^{CC}P_l^{CC}$ is almost vertical and in the plane $y = y_c(y_c$: the y coordinate of $P_c)$. Using the cross-sectional shape of the reconstructed 3D breast at $y = y_c$, the positions of P_u and P_l are calculated in the inverse manner to that described earlier.

We have 3 points(P_u,P_c and P_l) on the curve uncompressed from the straight line. The rest of the curve is estimated based upon **Approximation A4** as follows. Firstly, the vertical line P_0P_u (see Figure 5 for P_0) and its deformed curve due to CC-compression are obtained based on **A4** (the dotted lines in Figure 5). Applying uniform shrinking (stretching) as we assumed in **A3** we can see how each point on the compressed quadratic curve moves by uncompression (for example, $\nearrow$in Figure 5). The movement of each point on the line $P_cP_u^{CC}$ due to uncompression is estimated by assuming that it is the same as the point on the quadratic curve having the same z coordinate. For example, in Figure 5, P_i^{CC} is moved to P_i with translation of $\nearrow$. Although the distance from the reference point gets far as the z coordinate approaches 0, this does not lead to a big error however because the amount of displacement become smaller simultaneously. More specifically, from N points which are sampled from the line $P_cP_u^{CC}$ at regular intervals, the 3D coordinate sequence representing the curve P_cP_u is obtained. In the experiments in this paper, we take N equals to 100.

The following process details another way to calculate the 3D coordinate sequence representing the curve P_cP_u. While moving P from P_0 to P_c along the x-axis in steps of length $|P_0 - P_c|/N$,
1) The intersection of the vertical line through P and the upper breast contour, $P_u(P)$, and its corresponding point under compression $P_u^{CC}(P)$ are calculated.
2) The intersection of the quadratic curve fixed by the two points, P and $P_u^{CC}(P)$ and the vertical line $P_cP_u^{CC}$ is calculated.
3) The corresponding point to the intersection on the vertical line $PP_u^{CC}(P)$ is calculated. This is the uncompressed position of the intersection and added as a point of the point sequence representing the curve P_cP_u.

The three steps are iterated until P reaches P_c, that is N times. Though the latter process gives slightly more accurate results, it is quite slow and for this reason we currently adopt the earlier process.

The 3D coordinate sequence for P_cP_l is computed in the same way. By combining the two sequences, the 3D coordinate sequence $(x_k, y_k, z_k)(k = 1 \sim 2N + 1)$ is obtained which represents the curve P_uP_l.

C) Simulation of camera direction change

Both projection and compression can be considered simply using new rotated coordinates which set the camera and the compression direction along the z axis. First of all, the reconstructed 3D breast is rotated by $-\theta$ around the x-axis which has the same effect as changing the camera direction by θ. The nipple keeps the same coordinates after the rotation since it lies on the x-axis. Each point, $P_k(k = 1 \sim 2N + 1)$ on the reconstructed curve is transformed from (x_k, y_k, z_k) onto (x'_k, y'_k, z'_k).

D) Calculation of deformation by compression

For each point on the reconstructed curve $P'_k(x'_k, y'_k, z'_k)$ we perform the following, using the cross-section of the original breast in the plane $y' = y'_k$: Figure 6 shows an example of a case where P'_k lies above the plane $z' = 0$. From the coordinates of the intersection of the contour and the vertical line passing through $P'_k(x'_k, y'_k, z'_k)$, $P'_{u,k}$, the coordinate of its corresponding point on the contour of the compressed breast, $P''_{u,k}$ is calculated in the way described in **3.2**. Applying uniform stretch(shrink)(**A3**) to the deformation from the line $P'_{c,k}P'_{u,k}$ to the quadrant curve $P'_{c,k}P''_{u,k}$, $P''_k(x''_k, y''_k, z''_k)$ is determined on the curve $P'_{c,k}P''_{u,k}$. In the case of P'_k lying below the plane $z = 0$, $P'_{l,k}$ and $P''_{l,k}$ are calculated and used instead.

E) Projection onto the MLO image plane

The projected coordinates of the nipple and the relative points are:

$$i'^{MLO}_n = x_n(L/L^{MLO})/a,$$
$$j'^{MLO}_n = (y'^{MLO}_{source} + (y_n - y'^{MLO}_{source})(L/L^{MLO}))/a,$$
$$i'^{MLO}_k = x''_k(L/(L^{MLO} - z''_k))/a,$$
$$j'^{MLO}_k = (y'^{MLO}_{source} + (y''_k - y'^{MLO}_{source})(L/(L^{MLO} - z''_k)))/a.$$

Here, y'^{MLO}_{source} is the y' coordinate of the x-ray source, $L^{MLO} = L - H^{MLO}/2$ and a is the pixel size.

Since, in practice, the rotation axis of the x-ray system does not exactly coincide with the x axis, this causes a translation component. Additionally, a woman might change her position slightly relative to the x-ray system between the two images. To compensate for these translation effects, the projected line is registered in the MLO image so that the projected

nipple is superimposed on the nipple observed in the MLO image, whose coordinate is (i_n^{MLO}, j_n^{MLO}).

$i_k^{MLO} = i_k'^{MLO} + (i_n^{MLO} - i_n'^{MLO})$,
$j_k^{MLO} = j_k'^{MLO} + (j_n^{MLO} - j_n'^{MLO})$.

The resultant sequence of the image coordinate $(k = 1 \sim 2N + 1)$ represents the curved epipolar line on the MLO image for the point (i_s^{CC}, j_s^{CC}) on the CC image.

5 Results

5.1 Prediction of correspondence

In general, it is difficult even for clinicians to determine accurate correspondences between the CC and MLO images. However, clinicians can determine some correspondences with confidence, based largely on the similarity of the intensity patterns in the two images. We have gathered 37 lesions (in mammograms of 13 left breasts and 11 right breasts) whose correspondence between the CC and the MLO images was known in such a way and applied our method to the lesions. The camera angle for the MLO image is not currently recorded at the Oxford Breast Care Unit. Therefore, we use the best prediction from the simulations with camera angles of 45°, 52.5°, and 60°, since $45 - 60°$ contains the angular rotation between CC-MLO for almost all cases in practice. The minimum distance from the correct position to the resultant epipolar curves are measured and listed in Table 1.

Figure 7 shows a typical example (No.18 in Table1). The white square in the CC image is the given position of a lesion. The thick white solid line in the MLO is the curved epipolar line. The 3D reconstructed curves before and after simulation of MLO-compression in the new MLO coordinates are shown as a thin and a thick line respectively in Figure 8a. Figure 8b is a side view from the (0,1,0) direction. The dashed line shows the lower boundary of the breast under MLO-compression. Since, the lower part of the reconstructed 3D curve lies in the part of breast which deforms considerably because of being far from the mid-plane($z' = 0$), it moves substantially under MLO compression. As shown in Figure 7 the computed epipolar curve predicts quite accurately the position of the corresponding lesion which is marked with the cross.

For the same data, we asked two experienced radiologists to draw the region in the MLO images which they estimate to correspond to the marked position in the CC images. In the experiments, only the outlines of the breasts were given to the radiologists so that they could not use intensity information. Since they use lines to show the possible positions, the minimum distance from the correct position to the lines are measured and listed in Table 1. In Figure 7, the result of Radiologist 1 is illustrated as the dashed line and that of Radiologist 2 as the dotted line.

Radiologist 1 searched for the corresponding lesion along the vertical line having the same distance from the MLO nipple as the horizontal distance between the lesion and the nipple in the CC image. This equates to the ordinary epipolar line which is calculated from camera geometry without consideration of breast deformation. Since lesions move considerably by the compression especially when the lesion lies near the skin, the result of Radiologist 1 is often quite inaccurate (eg. No.5, 18 and 25 in Table 1).

Radiologist 2 uses inclined lines toward the nipple which has the same distance from the MLO nipple as the horizontal distance between the lesion and the nipple in the CC image. Since most lesions lie in the upper part of the breast (33/37 in our experiments) where the corresponding lines tend to be inclined so, the results of Radiologist 2 are often fairly good. However, when lesions lie in the lower part of the breast (No.1, 15, 19 and 20 in Table 1), Radiologist 2's minimum distance often becomes the largest among the three techniques. Additionally, although lesions tend to be moved toward the nipple by CC-uncompression, the lesions sometimes move substantially away from the nipple by MLO-compression depending on their positions. In these cases, Radiologist 2 has a large minimum distance (No.13, 14, 22 and 29 in Table 1).

We also compared with a typical prediction method used by many radiologists. It uses the circumference of the circle with its center at the MLO nipple and with a radius of the Euclidean distance between the lesion and the nipple on the CC image. The thin white line in Fig. 7 shows the result. The minimum distance from the correct position to the predictions are also measured and listed as R 3 in Table 1. The results show a similar tendency to R 2 but a little better.

As shown in the bottom line of Table 1, the average of the minimum distances resulting from using our method is 22.6 pixels, less than the radiologists' results which were 39.1 pixels and 29.4 pixels, 28.5 pixels.

Its standard deviation is also smaller than the others. This shows the practical usefulness of the method as a guide for finding the corresponding lesion in the MLO images.

To examine the effect of correct MLO angles, we measured the angles for several mammographic examinations. Table 2 show the results of the same experiments using the correct MLO angles. The results of our method using 45 and 60 degrees for MLO angles and of the typical prediction (R 3) are listed together for comparison. As shown in the table, the average distance using the correct MLO angle is smaller than that with incorrect MLO angles, as expected. Although the values using the correct MLO angle do not always give the minimum in the row, it is more important to stably predict closer positions when we use the prediction with some allowable error to search for real correspondences. Figure 9a and 9b respectively show examples which gives the best prediction(No.38 in Table 2) and the worst (No.45 $\sim$ 48 in Table 2).

5.2 Estimation of 3D position

The proposed method offers another possibility besides the prediction of the correspondence in the other image: it also can help to estimate the 3D position of a lesion in the uncompressed breast, despite the fact that the breast is never imaged in the uncompressed state in mammography. This technique works after finding the corresponding point along the epipolar curve and then back-tracking the movement of the point during the simulation of the processes shown in Figure 2b. Figure 10 shows an example using the x-rays of Figure 7. The red point in Figure 10a is the closest point on the epipolar curve to the real corresponding point. More specifically, the point is selected from the sequence of $2N + 1$ points presenting the epipolar curve which explained in Section 4 E). By back-tracking the change in the coordinates of the point through the processes E) $\rightarrow$ D) $\rightarrow$ C) $\rightarrow$ B) as shown in Figure 10b, it is deduced that the lesion lies at $(65.9, -33.3, 36.5)$(mm) in the breast coordinates as shown in 10c.

To examine the accuracy of the estimation, we applied our method to CC and MLO images of breasts which also have MRI data. Figure 11a shows x-ray images with the result of applying the proposed method to the images. Figure11b is one of the slices of MR which includes the lesion given in the CC image. The position of the lesion is marked with a red circle. The relative position of the lesion to the nipple is estimated as (-52.7, -23.7, 55.4)(mm) by the proposed method, while that obtained from the MR slice images is (-55.9, -25.8, 52.1)(mm). Figure 11c, d shows the positions respectively. The 3D shape in Figure 11d was reconstructed from the breast contour manually-extracted from the MR slice images, where only an upper part of the breast is taken. Since during MRI the breast is pendulous in specially designed breast coil (the patient lies on her front in the magnet), the breast shape is further distorted by gravity. In particular, the shape in the MRI machine is *not* the same as that used in the technique developed above, though it is similar. As we see in the numerical values and the figures, the resultant 3D position of the lesion coincides well with that of the MRI data. Although we have done only this comparison because of the difficulty to find a lesion in a breast which is observed both in mammogram and MRI scans, the accuracy in the estimation of the 3D position by our method can be expected to be within practically useful values.

6 Conclusion

In this paper, we have proposed an approach to calculating curved epipolar lines for matching a deformable object between time-varying stereo images. We implemented this approach to find correspondences between different view breast x-rays since this is an important practical case of the general problem. To analytically simulate the large deformation of the breast, we developed a simplified model of the deformation. The model appears adequate despite the fact that a number of coarse approximations were made. This probably reflects the careful consideration of the actual deformations taking place. The results are promising and appear to offer a useful aid to the radiologist or computer-system in determining the exact corresponding position by limiting the search area. Although we explained our method for the CC and the MLO images, the method is applicable for any directions.

A major practical use of our method is that once corresponding positions between the two views are found along the epipolar curve, the corresponding 3D position in the uncompressed breast can be determined. We compared the estimated result with the 3D position obtained from MR scans for the same breast. Although the number of experiments is not yet sufficient to firmly establish the accuracy of our method,

the early results are promising. This lesion localization is very important since it can be used to guide biopsies where necessary.

From the clinical view point, the work presented here will also help in understanding what exactly happens in 3D space as the breast is compressed. For example, our method can show the possible positions of a composite mass which is false positive lesion because of the accumulation of the tissues along a projection. Although we assume the criteria for performing a mammogram is kept, in practice, it is sometimes broken because of variations in breast shape and poor radiographic technique. We judge that this may be the cause of the big deviation in the results of No. 8, 9 and 35-37(the three lesions are in the same image) in Table 1. Further work will address this.

Future work might involve using tagged MRI to determine "ground truth" about the internal deformations of the breast with compression. Such information would enable us to improve on the model and might enable us to move to direct simulation of 3D deformation rather than dealing with 2D cross-sections. We have conducted a number of experiments with 3D finite element models. However, we find that building such finite element models, and simulating large breast deformations is intrinsically time-consuming. This poses a major problem in clinical practice, where rapid computation are necessary in order for an algorithm to be used. Of course, there is no point computing answers quickly if the results are unacceptable. However, we find that the slight extra accuracy gained by a finite element model does not warrant the significant addition in computation, particularly as it is not yet clear how to develop realistic finite element models that take account of the anisotropy of breast tissue, and the preponderance of Cooper's ligaments. That does not mean that our approximate model cannot be improved; indeed that is our major focus. We have, for example, begun to explore the idea of breast volume conservation[13][14]. We will also conduct work using the model presented here as an initial approximation which we will then improve using matching image features from the two images.

Acknowledgments

We are thankful to Basil Shepstone and Ruth English for their clinical advice, Paul Hayton and Niall Moore for their help in analyzing breast MR images and Margaret Yam for helping mammogram data acquisition. The first author thanks the STA's middle-term researcher sending programme and the Specific International Joint Research programme. She is also thankful to Dr. Tsukune, Dr. Tsukiyama, the members of Computer Vision group in ETL and the ETL administrators for their support of her research in the University of Oxford. She is grateful to Nobuyuki Kita for much useful advice and encouragement. RPH and JMB thank the EPSRC for supporting the work reported in this paper. JMB further acknowledges the EPSRC Senior Fellowship programme which gave him time to work on this project.

References

[1] J. Caseldine, R. Blamey, E. Roebuck, and C. Elston: *"Breast Disease for Radiographers"*, Wright, England, 1988.

[2] L. G. Brown: "A survey of image registration techniques", *ACM Computing Surveys*, Vol 24, No. 4, pp. 325–376, 1992.

[3] R. P. Highnam and J. M. Brady: *"Mammographic image processing"*, Kluwer Academic Publishing, 1999.

[4] O. D. Faugeras: *"Three-Dimensional Computer Vision"*, MIT Press, 1993.

[5] W. Spiesberger: "Mammogram inspection by computer", *IEEE Trans. on Biomedical Engineering*, **26**, 4, pp. 213–219, 1979.

[6] E. A. Sickles: "Practical solutions to common mammographic problems: tailoring the examination", *American Journal of Roentgenal*, Vol 2, No. 4, pp. 333–356, 1988.

[7] Y. Kita: "Elastic-model driven analysis of several views of a deformable cylindrical object", *IEEE trans. Pattern Anal. & Mach. Intell.*, **18**, 12, pp. 1150–1162, 1996.

[8] A. Singh, D. Goldgof, and D. Terzopoulos: *"Deformable models in medical image analysis"*, the IEEE Computer Society, 1998.

[9] J. Park, D. Metaxas and L. Axel: "Analysis of left ventricular wall motion based on volumetric deformable models and MRI-SPAMM", *Medical Image Analysis*, Vol. 1, No. 1, pp. 53–71, 1996.

[10] E. Roebuck: *"Clinical radiology of the breast"*, Heinemann medical books, Oxford, 1990.

[11] R. Novak: *"The transformation of the female breast during compression at mammography with special reference to the importance for localization of a lesion"*, ACTA radiologica supplement 371 Stockholm, 1989.

[12] R. P. Highnam, J. M. Brady and B. J. Shepstone: "Estimation of breast thickness in mammography", *British Journal of Radiology*, 1997.

[13] M. Yam, J. M. Brady, R. P. Highnam, R. E. English and Y. Kita: "Three-dimensional reconstruction of microcalcification clusters from two mammographic views", In *Proc. IWDM, Toronto, Canada*, pp., 2000.

[14] M. Yam, J. M. Brady, R. P. Highnam, R. E. English and Y. Kita: "Reconstructing microcalcification clusters in 3-D using a parametrised compression model", In *Proc. CARS 2000, San Francisco*, pp.723–728, 2000.

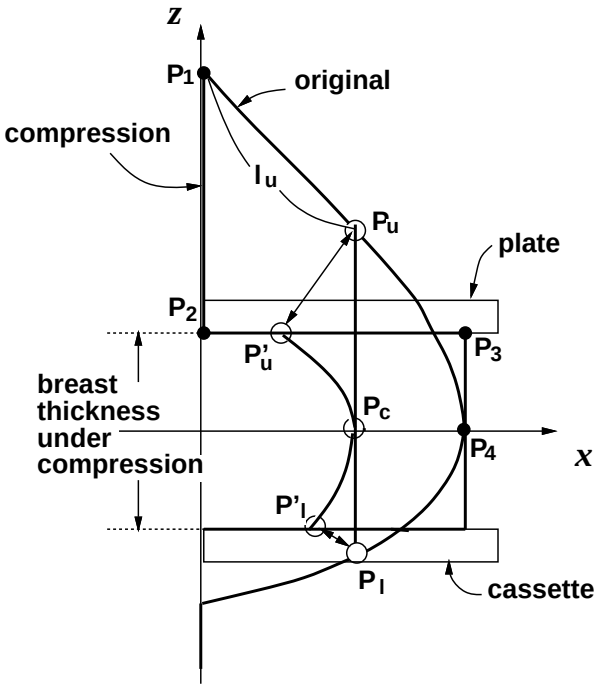

Figure 3: Schematic breast compression.(one cross-section for CC-compression)

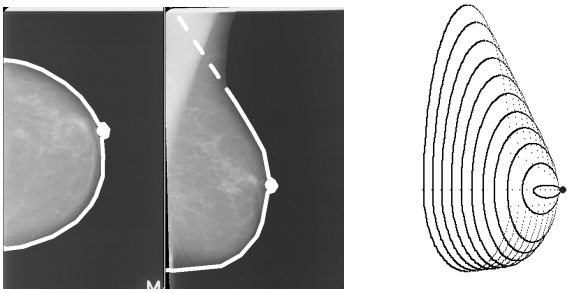

(a) CC image (b) MLO image (c)

Figure 4: 3D reconstruction of the breast

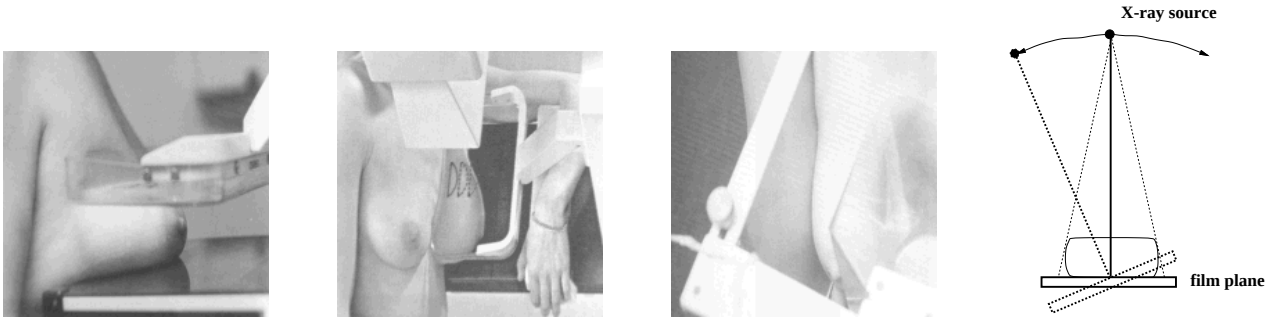

(a) (b) (c) (d)

Figure 1: Views of the breast: (a) cranio-caudal,(b) medio-lateral oblique, (c) medio-lateral and (d) schema of x-ray source movements[1].

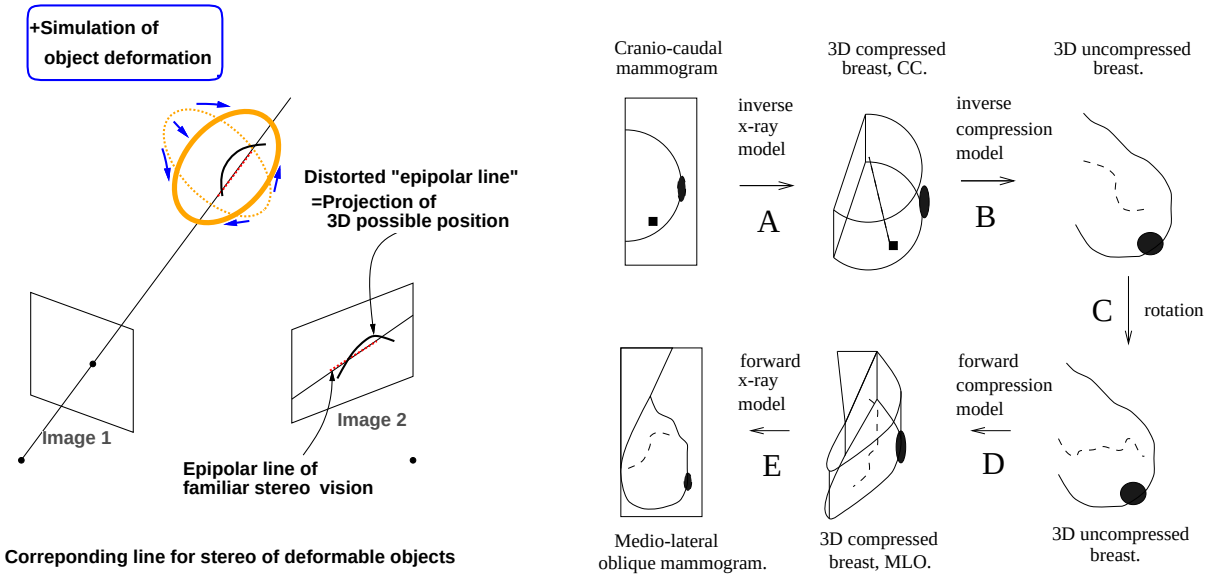

(a) Principle (b) Concrete stream in breast x-ray images

Figure 2: Strategy for determining correspondences of a deformable object imaged from different views.

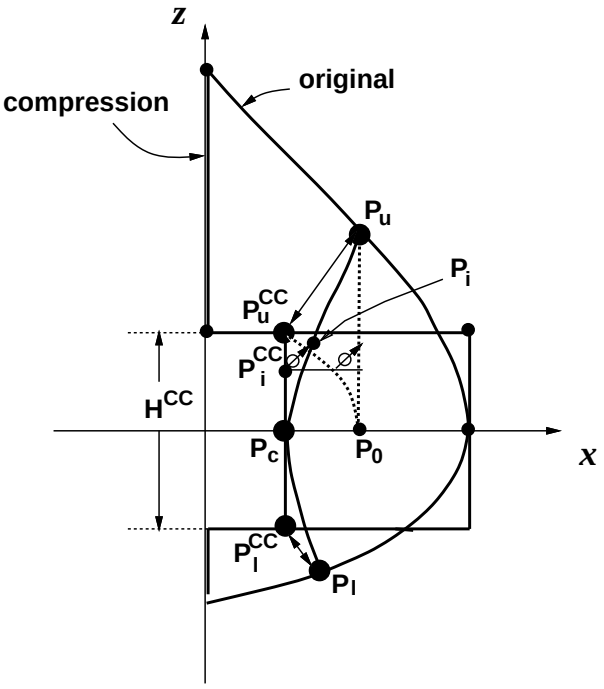

Figure 5: 3D reconstruction of corresponding curve in original breast(cross-section for CC-compression at $y = y_c$)

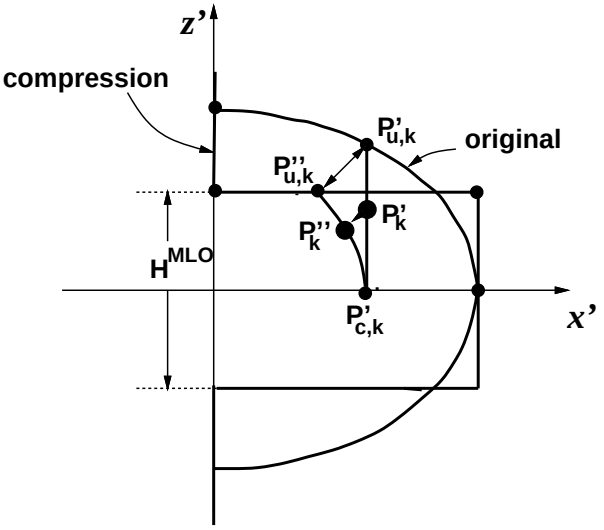

Figure 6: Estimation of movement of arbitrary point caused by MLO-compression (cross-section for MLO-compression at $y' = y'_k$).

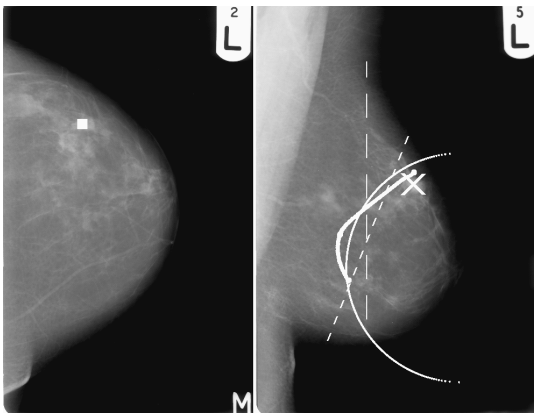

(a) CC image (b) MLO image

Figure 7: Example 1 of correspondence: the thick white curve shows the epipolar curve estimated by our method; the dashed and dotted lines are the corresponding estimates by Radiologists 1 and 2 respectively; the thin white curve shows the result of a typical prediction method used by many radiologists.

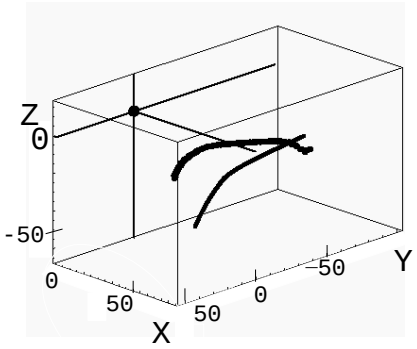

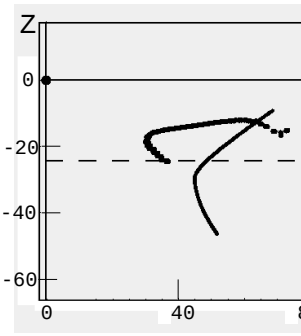

(a) (b)

Figure 8: 3D corresponding curve of the example in Figure 7: thin and thick lines are the corresponding line before and after the simulation of the MLO-compression respectively .

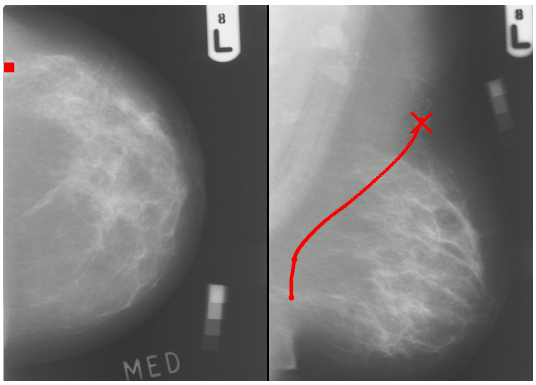

CC image MLO image

(a) No.38 in Table2

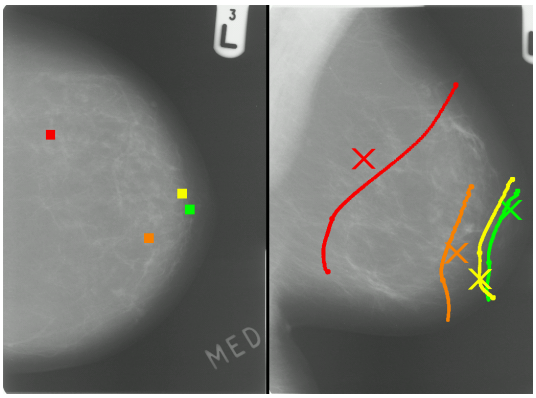

CC image MLO image

(b) No.45 $\sim$ 48 in Table 2

Figure 9: Example 2 of correspondences: the solid curves are the estimated epipolar lines using the correct MLO angles.

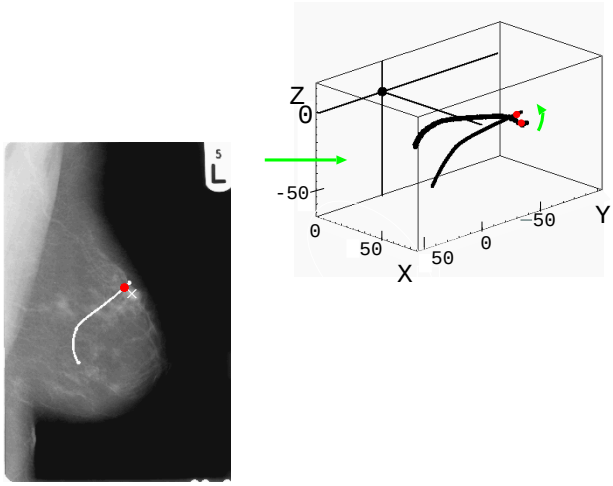

(a) (b)

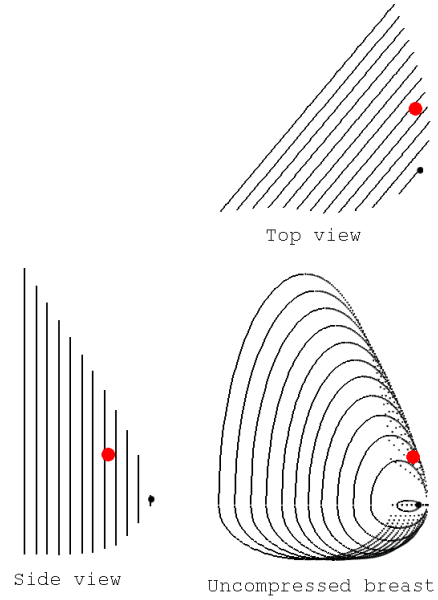

(c)

Figure 10: Example 1 of estimation of the 3D position of the lesion (red circle)

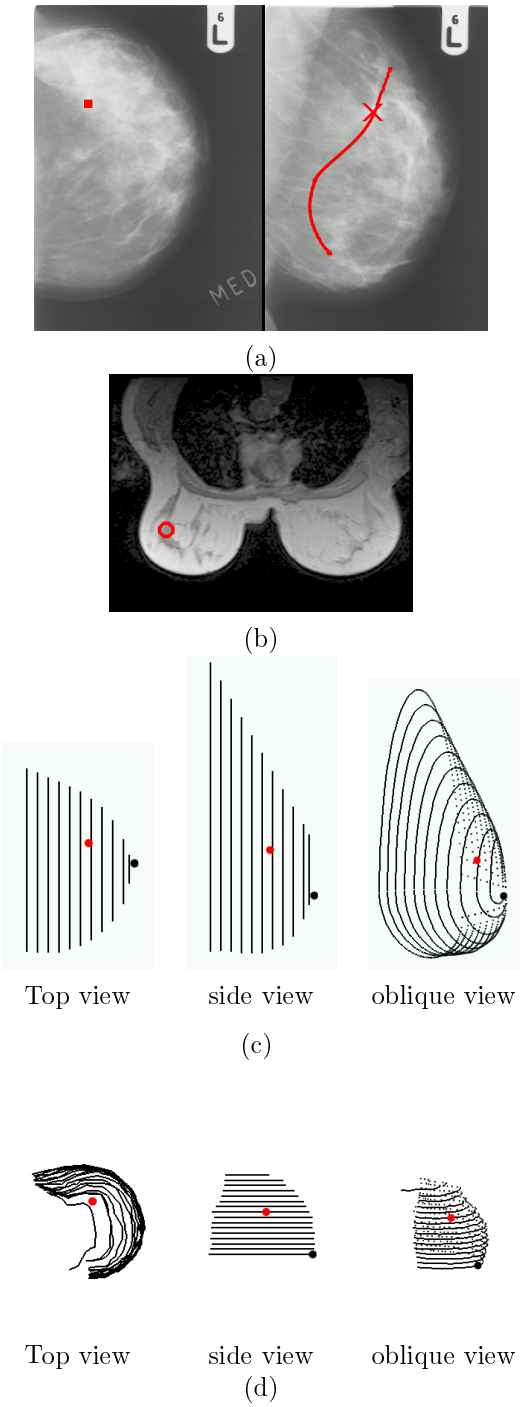

(a) (b) (c) (d)

Figure 11: Example 2 of estimation of the 3D position of the lesion (red circle)

Table 1 Minimum distance between the correct position and the resultant epipolar curve measured in pixels (0.3mm) in 512 × 720 images. KHB is the algorithm described in this paper.

No.	KH1	KH2	B3	KHB
1	0.2	11.0	31.0	15.6
2	30.6	22.0	22.4	11.7
3	38.2	35.0	24.1	39.6
4	32.7	10.0	8.5	17.6
5	13.4	95.0	5.5	18.9
6	2.9	47.0	27.8	25.0
7	5.2	5.0	6.6	4.3
8	92.6	99.0	99.6	114.8
9	59.5	81.0	46.0	83.2
10	18.7	32.0	2.9	8.9
11	1.0	1.0	28.4	35.1
12	5.9	4.0	1.7	14.1
13	37.5	1.0	71.5	47.2
14	34.7	41.0	57.6	14.8
15	7.7	9.0	21.1	11.0
16	6.3	11.0	2.9	9.0
17	30.6	9.0	54.9	67.6
18	17.4	88.0	41.6	34.8
19	0.3	5.0	19.0	5.5
20	19.0	41.0	16.9	3.6
21	18.0	31.0	18.8	9.1
22	32.6	27.0	76.9	25.0
23	0.2	5.0	7.3	5.1
24	26.1	43.0	4.5	46.5
25	1.4	93.0	22.7	32.4
26	24.9	9.0	10.6	11.4
27	26.7	10.0	24.5	20.6
28	18.5	21.0	20.0	8.1
29	17.2	35.0	71.9	12.4
30	10.3	7.0	24.8	39.5
31	5.8	10.0	2.4	6.4
32	32.7	53.0	51.1	40.3
33	0.9	61.0	26.9	5.3
34	31.7	34.0	38.3	62.7
35	42.7	102.0	40.4	66.9
36	54.9	117.0	18.5	34.6
37	37.1	142.0	36.9	44.9
Ave.	22.6	39.1	29.4	28.5
SD	19.5	37.3	23.3	24.9

Table 2 Minimum distance between the correct position and the resultant epipolar curve measured in pixels (0.3mm) in 512 × 720 images with MLO camera angle information. KHB is the algorithm described in this paper.

No.	MLO angle (deg.)	KHB with correct angle.	KHB with 60 deg.	KHB with 45 deg.	R 3
38	55	2.7	12.5	47.5	24.4
39	50	2.7	4.6	1.2	14.1
40	50	4.9	6.3	9.0	19.8
41	50	9.7	10.6	9.2	8.7
42	50	5.2	4.2	5.6	5.7
43	50	14.0	10.0	16.4	8.9
44	50	36.1	37.2	35.5	37.7
45	55	41.4	40.6	42.5	3.3
46	55	9.3	6.3	14.7	39.5
47	55	2.0	3.4	3.6	6.9
48	55	20.7	21.0	20.3	31.8
Ave.		13.5	14.2	18.7	18.3
SD		13.1	12.6	15.4	12.6